Pipe Burst Risk State Assessment and Classification Based on Water Hammer Analysis for Water Supply Networks

Ronghe Wang[1]; Zhixun Wang[2]; Xiaoxue Wang[3]; Haibo Yang[4]; and Jilong Sun[5]

Abstract: Hydraulic transients pose many risks to urban water distribution systems. The high pressure induced by a hydraulic transient can cause pipe bursts, the negative pressure can cause pipe collapses, cavitation can cause pipeline erosions and pump impeller damages, and the transient forces can loosen pipe joints. We derived the hydraulic calculating equations based on the method of characteristics (MOC) by considering the pipe head loss and node cavitation. Four individual factors and one composite factor for hydraulic transient risk are presented along with the method of calculation of the indicators. They can produce a tabular result that is color coded by risk, and the risk classification map can be built by a four-layer state assessment and color coding technology. They are Class I with green for safe level, Class II with cyan for warning level, Class III with blue for dangerous level, and Class IV with red for severe level. The pipe burst risk assessment methods and procedures are presented. Finally, a sample model and a Chinese city pipe network system are presented for pipe burst risk classification examples. **DOI: 10.1061/(ASCE)WR.1943-5452.0000404.**

Author keywords: Water distribution network; Modeling; Water hammer; Pipe burst; State assessment; Risk classification.

Introduction

Pipe burst is one of the key issues that affect urban water distribution systems, and can lead to water supply interruption, loss of lives, property damage, and water quality problems. If the time of the pipe burst incidents can be anticipated beforehand, a pipe network maintenance plan can be formulated in advance to avoid the accidents.

Pipe bursts can be broadly attributed to hydraulic and nonhydraulic factors. The hydraulic factors are the hydraulic transient shock and cavitation caused by the operation of pumps and valves. The nonhydraulic factors include pipe stress, pipe corrosion, the quality of construction, foundation failure, etc.

For hydraulic factors, the vaporization phenomenon occurs when the pressure inside the pipe falls below the vapor pressure of the water; this will form a water hammer with water column separation and cavitation. The water hammer produced as a result of cavitation is different from the one from a traditional pump and valve opening or closing on the mechanism, and the current water hammer protection devices cannot function effectively (Xiong et al. 2003). In addition, the air sucked in by the exhaust valves, the water vapor generated by the negative pressure, as well as the air separated out from the water, will be compressed at the top of the pipe. The air can be divided into dispersion airbags by the surge, which will cause the pipe pressure to oscillate and shock the wall continuously, eventually resulting in pipeline damage. Air valves can resolve the problems in the pipes. The main reason for pipe bursts is due to a lack of air valves or air valve failures.

In terms of nonhydraulic factors, underground pipelines will suffer from longitudinal and circumferential tensile stress, circumferential bending and socket cracking stress due to overburden pressure, water pressure, and temperature changes (Kim et al. 2012). For example, changes in environment and water temperature will cause expansion or contraction in the pipeline and make the rigid pipe joints crack due to the huge tensile stress. The water mains may be broken due to bending axial stress under the load of the walls or centralized weight. Soil displacement has a greater impact on the large-diameter pipes, and could easily lead to cracking of the pipe socket. The groundwater quality and soil composition will produce electrochemical corrosion to the metal pipes. The stray current induced by the high-voltage power lines and subway will accelerate corrosion of the steel pipes. The dissolved gases in the water will be separated from the water and react with the metal wall to form a large number of fine cracks, leading to corrosion of the pipe walls. The corrosion can cause wall thinning, leading to the reduction in strength of the pipe, and could easily produce a pipe burst incident (Rajani and Kleiner 2013).

For research on hydraulic transient, from the mathematical derivation of the eighteenth century, to the graphical analysis of the mid-twentieth century, and up to the current computer digital simulation, significant progress has been made to the advancement of the field. One of the major achievements has been establishing the relationship between the multiphase and multicomponent transient flow state equation and wave velocity, water hammer equations, and control equations, such as the Joukowsky equation, one-dimensional (1D) water hammer equations, two-dimensional (2D), and quasi-2D plane wave equations (Ghidaoui et al. 2005). Based on the transient flow simulation theory, Colombo et al.

[1]Professor, Key Clean Production Laboratory, Graduate School at Shenzhen, Tsinghua Univ., Shenzhen, Guangdong 518055, China (corresponding author). E-mail: Wang.ronghe@sz.tsinghua.edu.cn

[2]M.E. Student, Rensselaer Polytechnic Institute, Troy, NY 12180. E-mail: andw90@hotmail.com

[3]M.S. Student, Key Clean Production Laboratory, Graduate School at Shenzhen, Tsinghua Univ., Shenzhen, Guangdong 518055, China.

[4]M.E. Student, Key Clean Production Laboratory, Graduate School at Shenzhen, Tsinghua Univ., Shenzhen, Guangdong 518055, China.

[5]Ph.D. Student, Key Clean Production Laboratory, Graduate School at Shenzhen, Tsinghua Univ., Shenzhen, Guangdong 518055, China.

Note. This manuscript was submitted on April 1, 2013; approved on August 20, 2013; published online on August 23, 2013. Discussion period open until August 19, 2014; separate discussions must be submitted for individual papers. This paper is part of the ***Journal of Water Resources Planning and Management***, © ASCE, ISSN 0733-9496/04014005(8)/$25.00.

(2009) proposed an aqueducts fault detection technology, Lee et al. (2007) proposed the pipe network leak and deterioration over time detection technology by time domain reflectometry (TDR), Arbon et al. (2007) proposed a pipeline corrosion and blockage detection technology, Stephens et al. (2011) proposed a cement mortar lining spalling detection technology, Zamanzadeh et al. (2007) analyzed the risk of water pollution, burst pipe, and clogging, and Gong et al. (2013) proposed a detection technology for pipe friction, wall thickness, velocity, position, and pipe length.

The early warning system is mainly composed of four layers, namely, an information collection layer, data transport layer, data processing layer, and application layer. It is widely used in other industries outside the water industry, such as weather, geological disasters, and disease plague control fields, e.g., the Famine Early Warning System (FEWS). The Consortium of Universities for the Advancement of Hydrologic Science. Hydrologic Information System (CUAHSI HIS) has established a mechanism for storing, publishing, sharing, and exploring the hydrological data under the support of the U.S. National Science Foundation. It contains the data from 1.96 million monitoring points of American rivers. The U.S. EPA, the U.S. National Bureau of Geology and more than 100 large monitoring agencies have registered and provide data services (Horsburgh et al. 2009). The Environmental Protection Ministry of China has established 100 automatic water quality monitoring stations at seven major rivers. Some local governments and universities in China also have established regional early warning systems under the support of major national science and technology water projects, such as the East River raw water three-layer early warning system, which is used in China in the city of Dongguan (Zhang et al. 2012). In the water-distribution-system field, Ostfeld and Salomons (2004) presented a methodology for getting the optimal layout of an early warning detection system for terrorist hazard intrusion by genetic algorithm framework integrated with the software program *EPANET* (Rossman 2000). Kroll (2010) analyzed the methods and criteria for evaluating early warning systems for water quality problems. Mutikanga et al. (2013) analyzed the methods and tools for managing water losses.

For the research on pipe burst risk assessment, Romano and Kapelan (2011) presented a burst or leakage locating method based on district metered area (DMA) with real-time pressure and flow sensors and artificial intelligence technologies. Ebacher et al. (2011) presented a technology to assess the public health risk by transient analysis of negative pressure in water distribution systems. Livingston et al. (2012) presented a method to evaluate the condition of the ductile iron pipe based on the study of the Underwood Creek force main, Milwaukee metropolitan sewerage district. Kanta and Brumbelow (2013) presented a method that integrated failure probability, risk analysis, and optimization of risk that can be used to assess system vulnerabilities and potential mitigation actions. Grigg (2013) proposed a risk-assessment formulation of the decision process for pipeline replacement based on the research of professional, economic, and political leadership and asset management.

Basic Theory of Water Hammer and Problem Solving

Since the birth of Newtonian mechanics theory, Lagrange, Euler, and other scientists have done groundbreaking research on the theory of acoustic wave propagation in air and water through experiment. Monge proposed a method of characteristics (MOC) in 1789, Joukowsky proposed the water hammer forecast equation in 1904, and Wood, Streeter et al. derived the MOC controlling equations that can be used for computer programming in 1960s. Combining the above basic water hammer equations with the pipe energy equations, the node continuity equations, the pump characteristic curve equations, and the water hammer protection facilities' characteristic equations, the basic programmable MOC equation was derived as follows (Wang et al. 2011, 2013):

$$H_i + \alpha_i Q_i = h_i + \alpha_i q_i \tag{1}$$

in which capitalized letters represent the values at the current node and current time-step, lowercase letters represent the values of the adjacent nodes at the previous time-step. H and h are water head, meter (m); Q and q are pipe water flow, cubic meters per second (m^3/s). $\alpha = a/gS$, a is the acoustic wave speed in water, meter per second (m/s); S is the cross-sectional area of the pipe, in square meters (m^2).

When the pressure falls below the vaporization pressure at the water temperature of the current time, the vaporization phenomenon occurs. It will form a water hammer of water column separation and cavities collapsing. The vapor volume calculation formula at the nodes and midpoints of pipeline is

$$X = \sum X_i, \quad \text{and} \quad \frac{dX_i}{dt} = -Q_i \tag{2}$$

in which X is the vapor volume, m^3 and i is the index of pipes that connected to the node.

Solving the above problems is very complex. The correct results cannot be directly obtained by solving the equations because a lot of assumptions, boundary conditions, and a large number of digital computations are needed. To improve the computing speed and adapt to the large-scale pipe network, problem solving is divided into three levels.

When we ignore the pipe head loss and node cavitation, we assume the pipe friction factor $f_i = 0$, and water head $H = H_i$. This is a special case in which the friction losses of branches are zero based on the unsteady friction calculations, or the simplified education cases

$$AH = B \tag{3}$$

in which, $A = \sum 1/\alpha_i$ and $B = \sum(h_i/\alpha_i + q_i)$.

When considering only the pipe head loss, but not the node cavitation, the problem can be solved through an iterative process; the iterative formulas are as follows. This is a general case when the cavitation does not happen in the node based on the calculation results of the previous time step

$$AH^{(k)} = B - C^{(k-1)} \tag{4}$$

$$H_i^{(k)} = H^{(k)} + f_i Q_i^{(k-1)} |Q_i^{(k-1)}| \tag{5}$$

$$C^{(k-1)} = \sum (f_i/\alpha_i) Q_i^{(k-1)} |Q_i^{(k-1)}| \tag{6}$$

When considering both pipe head loss and node cavitation, we assume the node as the fixed head junction. The problem is still solved through an iterative process, and the iterative formula is as follows. This is the most common case for the node having cavitation based on the calculation results of previous time step

$$X_i^{(k)} = X_i^{(k-1)} - 1/2\Delta T(Q_i^{(k)} + Q_i^{(k-1)}) \tag{7}$$

in which ΔT is the time step, s.

Risk of Water Hammer State Assessment

Compiling data collected from GIS, construction drawings, water consumption records, pipe burst records, and other water supply network information, the physical information of the pipe network is converted into digital data, and the computerized pipe network model is established. The model is connected to the real-time monitoring system, a regular meter reading system, and the running and historical record database. After validating the parameters with the collected data, the model is ready to use for transient flow simulations. The next step is to design scenarios that could trigger the hydraulic transient. The scenarios include pump startup and shutdown, valve opening and closing, pipelines flushing, fire accidents, and large user overhauls, etc. Next, the model is run based on the designed scenarios, the results of computation are extracted, and a comprehensive analysis of the simulation results is conducted. The analysis includes the calculation of all the risk factors of pipe burst, and sending the data back to model with user data extension function. Finally, the pipe network risk map is created with color coding in the model. The map can provide decision-making references to the water supply network operation and maintenance.

After getting the maximum and the minimum water pressure, and the maximum vapor volume of each pipe and each node, and the impact force of each node, the pipe burst risk to the water supply network was evaluated from the following six aspects.

Risk Factor of Maximum Water Pressure of Each Node and Each Pipe

Pipe burst risk due to water pressure depends on two aspects, namely, the maximum water pressure and the designed safety pressure of each pipe. Depending on the pipe materials, the pipe wall thickness, and the production process, the designed safety pressure of the pipe is not fixed. The pipe burst risk because of high-pressure is calculated as the following formulas:

$$P_{\max} = \max(P_1, \ldots, P_i) \tag{8}$$

$$R_1 = (P_{\max} - P_b)/P_b, \quad \text{when } R_1 < 0, \qquad R_1 = 0 \tag{9}$$

where R_1 is the pipe burst risk factor based on water pressure. $P_{\max}$ is the maximum pressure of each pipe and each node among the scenarios calculated by hydraulic transient simulation, megapascals (MPa). P_b is the design safety pressure of each pipe or each node, MPa. P_i is the maximum pressure of each pipe and each node of the scenario i calculated by hydraulic transient simulation, MPa.

The designed safety pressure P_b can be obtained using the following:

1. When you have the design information, the design pressure can be used. But pipe corrosion and service time will still need to be considered;
2. It can be calculated by the following equation for metal pipes according to the diameter and wall thickness

$$P_b = \frac{2(\sigma E S)}{D + S} \tag{10}$$

where σ is the pipe material's allowable stress at the design temperature, MPa. E is the welded joints coefficient, normally 0.8. S is the thickness of a pipe wall in millimeters (mm). D is the pipe diameter in mm; and

3. It can be the calculated based on the extended period simulation (EPS) of the steady state simulation. Using $P_b = 1.25 \times$ maximum calculated pressure.

Risk Factor of Maximum Vacuum of Each Node and Each Pipe

$$P_{\min} = \min(P_1, \ldots, P_i) \tag{11}$$

$$R_2 = P_{\min}/P_v, \quad \text{when } R_2 < 0, \qquad R_2 = 0 \tag{12}$$

where R_2 is the pipe burst risk factor based on vacuum. $P_{\min}$ is the minimum calculated pressure among the scenarios, MPa. P_v is the maximum vacuum, and generally -0.1, MPa. P_i is the minimum pressure of the scenario i, MPa.

Risk Factor of Maximum Vapor Volume of Each Node and Each Pipe

$$V_{\max i} = \max(V_{1j}, \ldots, V_{ij}) \tag{13}$$

$$V_{\max} = \max(V_{\max 1}, \ldots, V_{\max i}) \tag{14}$$

$$R_3 = \mathrm{V}_{\max i}/\mathrm{V}_{\max} \tag{15}$$

where R_3 is the pipe burst risk factor based on vapor volume. V_{ij} is the calculated vapor volume of node j or pipe j under scenario i, m^3. $V_{\max i}$ is the maximum calculated vapor volume of scenario i, m^3. $V_{\max}$ is the maximum calculated vapor volume of the entire network of the nodes or the pipes, m^3.

Risk Factor of Maximum Transient Force of Each Node

$$F_{\max} = \max(F_1, \ldots, F_i) \tag{16}$$

$$R_4 = (F_{\max} - F_b)/F_b, \quad \text{when } R_4 < 0, \qquad R_4 = 0 \tag{17}$$

where R_4 is the pipe burst risk factor based on transient force of a node. $F_{\max}$ is the maximum calculated transient force among the scenarios, newton (N). F_b is the base of the impact force of each

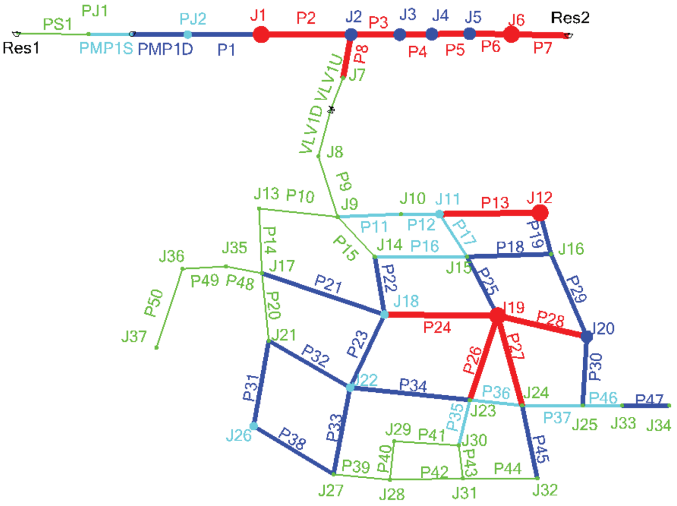

Fig. 1. (Color) Pipe burst risk color coding map for example 1

node, N. F_i is the maximum transient force of each node of the scenario i, N. F_b can be the maximum calculated impact force based on the steady state simulation. $F_b = 1.25 \times$ maximum calculated impact force of steady state.

Composite Pipe Burst Risk Factor of a Node or a Pipe

Once we get the risk factors for every node and pipe, we can classify the pipe burst risk by calculating the composite risk factors. As the examples demonstrate, two methods are proposed to obtain the composite factor.

1. Maximum risk factor

$$R = \max(R_1, \ldots, R_n) \tag{18}$$

where R is the composite pipe burst risk factor a node or a pipe. R_i is the i-th risk factors of pipe burst. n is the number of risk factors. For a node, $n = 4$; for the pipe, $n = 3$. Maximum positive pressure, negative pressure, vapor, and transient force are all the pipe bur factors; therefore this method can be used for comprehensive analysis of the pipe network system.

2. Composite risk factor

$$R = \sum_{i=1}^{n} (W_i R_i) \tag{19}$$

$$\sum_{i=1}^{n} W_i = 1 \tag{20}$$

where W_i is the weight of pipe burst risk factor i, and the sum of the weights of a node or a pipe is 1. W_i varies with the pipe materials and the local pipe networks. For example, prestressed concrete cylinder pipes (PCCP) can stand the negative pressure well, therefore W_2 can be 0. However, polyethylene (PE) pipes can be flattened by the negative pressure easily, therefore W_2 should be 0.5. If the user does not have any information about the network, one can use W_i as 0.25 for nodes and 0.33 for pipes. The W_i values will affect the risk factors and the pipe burst risk analysis results.

Table 1. Pipe Burst Risk State Assessment on Nodes without Protection

Node label	Elevation (m)	Pressure (steady state) (m)	Force (steady state) (kN)	Minimum pressure (transient) (m)	Maximum pressure (transient) (m)	Vapor (transient) (L)	Force (transient) (kN)	R1	R2	R3	R4	R
J1	412.0	50.6	576.8	−10.0	169.4	840.8	599.3	1.7	1.0	0.6	0.0	0.8
J2	395.0	66.1	1,164.5	−10.0	190.6	0.7	1,232.8	1.3	1.0	0.0	0.1	0.6
J3	395.0	65.0	424.6	−10.0	198.5	13.6	429.7	1.4	1.0	0.0	0.0	0.6
J4	386.0	73.0	509.3	−10.0	213.0	0.6	513.4	1.3	1.0	0.0	0.0	0.6
J5	380.0	77.6	524.3	−10.0	244.4	0.2	569.0	1.5	1.0	0.0	0.1	0.7
J6	420.0	36.6	325.6	−10.0	188.6	2.0	329.9	3.1	1.0	0.0	0.0	1.0
J7	395.0	63.2	391.1	−2.2	115.0	0.0	392.4	0.5	0.2	0.0	0.0	0.2
J8	395.0	63.2	240.4	−2.4	114.9	0.0	253.6	0.5	0.2	0.0	0.1	0.2
J9	395.0	61.4	430.0	8.7	88.4	0.0	435.4	0.2	0.0	0.0	0.0	0.0
J10	395.0	60.8	54.6	−0.8	126.9	0.0	57.4	0.7	0.1	0.0	0.1	0.2
J11	410.0	45.6	156.7	−5.2	110.9	0.0	168.4	1.0	0.5	0.0	0.1	0.4
J12	420.0	35.3	131.7	−10.0	131.5	0.7	167.2	2.0	1.0	0.0	0.3	0.8
J13	390.0	65.2	202.5	16.9	138.3	0.0	239.6	0.7	0.0	0.0	0.2	0.2
J14	396.0	59.3	194.1	0.4	125.2	0.0	200.9	0.7	0.0	0.0	0.0	0.2
J15	397.0	58.2	281.9	2.8	124.1	0.0	287.8	0.7	0.0	0.0	0.0	0.2
J16	397.0	58.1	226.7	1.0	126.2	0.0	241.0	0.7	0.0	0.0	0.1	0.2
J17	380.0	74.6	358.2	28.8	124.2	0.0	362.4	0.3	0.0	0.0	0.0	0.1
J18	420.0	34.6	356.5	−3.9	94.8	0.0	358.2	1.2	0.4	0.0	0.0	0.4
J19	435.0	19.6	279.5	−10.0	107.5	1,478.5	282.7	3.4	1.0	1.0	0.0	1.4
J20	410.0	44.5	158.0	−9.0	123.2	0.0	178.0	1.2	0.9	0.0	0.1	0.6
J21	385.0	67.1	185.8	14.6	130.5	0.0	187.8	0.6	0.0	0.0	0.0	0.1
J22	395.0	57.3	255.0	−5.7	116.2	0.0	255.9	0.6	0.6	0.0	0.0	0.3
J23	396.0	56.4	186.1	3.5	114.7	0.0	187.3	0.6	0.0	0.0	0.0	0.2
J24	397.0	55.4	163.2	11.0	114.1	0.0	164.8	0.7	0.0	0.0	0.0	0.2
J25	408.0	44.6	85.7	3.4	103.2	0.0	90.0	0.9	0.0	0.0	0.1	0.2
J26	390.0	60.3	140.3	−2.9	154.1	0.0	148.9	1.0	0.3	0.0	0.1	0.4
J27	395.0	53.9	171.2	21.9	94.6	0.0	174.7	0.4	0.0	0.0	0.0	0.1
J28	396.0	53.2	79.1	15.1	100.8	0.0	84.5	0.5	0.0	0.0	0.1	0.2
J29	396.0	53.3	51.4	8.9	94.0	0.0	61.3	0.4	0.0	0.0	0.2	0.2
J30	396.0	53.7	100.8	14.8	102.2	0.0	102.2	0.5	0.0	0.0	0.0	0.1
J31	396.0	53.3	93.9	12.9	103.5	0.0	97.8	0.6	0.0	0.0	0.0	0.2
J32	397.0	52.0	103.2	17.8	82.1	0.0	107.7	0.3	0.0	0.0	0.0	0.1
J33	410.0	41.8	100.5	3.5	99.9	0.0	101.0	0.9	0.0	0.0	0.0	0.2
J34	420.0	29.1	77.5	2.3	57.2	0.0	78.7	0.6	0.0	0.0	0.0	0.2
J35	372.0	81.5	61.7	25.2	130.6	0.0	62.1	0.3	0.0	0.0	0.0	0.1
J36	360.0	92.4	70.0	36.0	152.9	0.0	82.2	0.3	0.0	0.0	0.2	0.1
J37	355.0	96.3	42.7	38.4	166.1	0.0	59.6	0.4	0.0	0.0	0.4	0.2
PJ1	363.0	19.8	140.8	6.2	39.3	0.0	142.7	0.6	0.0	0.0	0.0	0.2
PJ2	363.0	99.8	166.9	−6.5	220.6	0.0	201.1	0.8	0.7	0.0	0.2	0.4

J. Water Resour. Plann. Manage. 2014.140.

Pipe Burst Risk Level Classification

Pipe burst risk can be classified using the four-layer state assessment division mechanism. There is a safe level, warning level, dangerous level, and severe level. Green indicates a value less than 0.25 for the given factor and therefore no warning. Cyan indicates 0.25–0.5 for a warning level, which means that regular inspections need to be conducted. Blue indicates 0.5–0.75 for a dangerous level, which means a high degree of concern is needed. Red indicates greater than 0.75 for a severe level, which means that technical measures need to be taken immediately.

Cases Studies

Example 1

As shown in Fig. 1, the pipe network system contains 62 pipes, 39 nodes, 2 reservoirs, 1 water pump, and 1 flow control valve. There are not any air valves or other hammer protection equipment installed in the system. The total pipe length is 13.261 km. The maximum diameter is 600 mm and the minimum diameter is 200 mm. The urban water consumption is 22,896 m^3/day.

Transient results were generated using *HAMMER* (Haestad Methods Water Solutions 2013) and they were exported to a program where the risk factors were calculated. These values were imported back into *HAMMER* for color coding display by creating a new pipe property using a "user-data extension" to display the risk factors.

For predicting the pipe burst risk of a water hammer, a pump shutdown scenario is simulated as running smoothly for 5 s, and then the valve is closed in 1 s. W_i is 0.25 for nodes and 0.33 for pipes. Table 1 shows the water hammer risk state assessment results for the nodes, and the results for pipes are shown in Table 2. The factors R, R_1–R_4 of nodes and pipes were imported into *HAMMER* by user data extension, and a color-coded map was created. The composite pipe burst risk classification map is shown in Fig. 1.

Results Analysis of Example 1

Using Tables 1 and 2, color-coded maps of R1, R2, R3, and R4 can be created. The maps can be used to intuitively analyze the burst risk for each pipe in the network system. Under normal circumstances, the color-coded map of the composite risk factor is sufficient for water hammer analysis.

As shown in Tables 1 and 2, many R1s are larger than 0.25, which means that the pipes are at a great risk of pipe burst, so R1 is an important risk factor for the system. For pipes that can withstand negative pressure, such as PCCP pipes, R2 is not a risk factor. But for pipes that cannot withstand negative pressure, such as PE pipes, R2 is very important. R3 has little impact on the entire system, but has severe level impact for points of J1 and J19. R3 indicates that the locations are under great risk of negative pressure and cavitation. R4 has little impact on moving the pipelines in example 1. But if there are no thrust restraints on the bends for the large water distribution systems, it is a very important risk factor.

From Fig. 1 and Table 1, we can find that the line from J1 to Res2 is a long-distance water main, which is usually the location where a water hammer occurs, and the pipe burst risk analysis produces the same results as the traditional hydraulic transient knowledge. As J1 and J6 are at higher points along the line, and their design safety pressures are lower, J1 and J6 rated as severe level is reasonable. J12 is on the edge of the water supply system, which reflects the hydraulic transient wave; it is also located on a higher elevation, which means the probability of negative pressure is higher; additionally it is at a bending point that changes the direction of the water flow; therefore, J12 classified as a severe location is reasonable. J19 is the point of highest elevation of the whole water supply system, which means negative pressure and vapor can form easily; therefore, J19 classified as the severe

Table 2. Pipe Burst Risk State Assessment on Pipes without Protection

Pipe label	Maximum pressure (transient) (m)	Minimum pressure (transient) (m)	Vapor (transient) (L)	Pressure (steady state) (m)	R1	R2	R3	R
P1	220.6	−10.0	20.9	100.5	0.8	1.0	0.0	0.6
P2	190.6	−10.0	839.1	66.6	1.3	1.0	1.0	1.1
P3	225.6	−10.0	15.8	66.6	1.7	1.0	0.0	0.9
P4	214.0	−10.0	52.9	73.4	1.3	1.0	0.1	0.8
P5	244.5	−10.0	4.2	77.7	1.5	1.0	0.0	0.8
P6	244.4	−10.0	4.3	77.7	1.5	1.0	0.0	0.8
P7	188.6	−10.0	7.7	36.7	3.1	1.0	0.0	1.4
P8	205.0	−10.0	1.9	66.6	1.5	1.0	0.0	0.8
P9	114.9	−2.4	0.0	63.4	0.5	0.2	0.0	0.2
P10	138.3	8.7	0.0	65.1	0.7	0.0	0.0	0.2
P11	126.9	−5.5	0.0	61.5	0.7	0.6	0.0	0.4
P12	126.9	−5.2	0.0	60.9	0.7	0.5	0.0	0.4
P13	132.0	−10.0	1.1	45.6	1.3	1.0	0.0	0.8
P14	143.7	16.4	0.0	74.4	0.6	0.0	0.0	0.2
P15	125.2	0.4	0.0	61.5	0.6	0.0	0.0	0.2
P16	133.0	−5.2	0.0	59.2	0.8	0.5	0.0	0.4
P17	124.1	−5.7	0.0	58.1	0.7	0.6	0.0	0.4
P18	126.2	−8.1	0.0	58.1	0.7	0.8	0.0	0.5
P19	133.7	−10.0	0.7	58.1	0.8	1.0	0.0	0.6
P20	146.9	12.4	0.0	74.4	0.6	0.0	0.0	0.2
P21	149.2	−10.0	0.1	74.4	0.6	1.0	0.0	0.5
P22	130.8	−10.0	0.1	59.2	0.8	1.0	0.0	0.6
P23	116.2	−10.0	0.2	57.0	0.6	1.0	0.0	0.5
P24	120.0	−10.0	466.8	34.5	1.8	1.0	0.6	1.1
P25	140.7	−10.0	250.1	58.1	0.9	1.0	0.3	0.7
P26	140.8	−10.0	347.4	56.1	1.0	1.0	0.4	0.8
P27	140.0	−10.0	335.0	55.2	1.0	1.0	0.4	0.8
P28	133.0	−10.0	182.3	44.4	1.4	1.0	0.2	0.9
P29	128.5	−10.0	0.1	58.1	0.8	1.0	0.0	0.6
P30	123.2	−10.0	0.1	44.4	1.2	1.0	0.0	0.7
P31	159.1	−8.7	0.0	66.8	0.9	0.9	0.0	0.6
P32	142.1	−10.0	0.4	66.8	0.7	1.0	0.0	0.6
P33	130.5	−10.0	0.0	57.0	0.8	1.0	0.0	0.6
P34	149.2	−10.0	0.1	57.0	1.1	1.0	0.0	0.7
P35	114.7	−3.5	0.0	56.1	0.6	0.4	0.0	0.3
P36	143.1	−4.3	0.0	56.1	1.0	0.4	0.0	0.5
P37	139.6	0.2	0.0	55.2	1.0	0.0	0.0	0.3
P38	154.1	−10.0	0.0	59.8	1.1	1.0	0.0	0.7
P39	104.7	10.0	0.0	53.1	0.6	0.0	0.0	0.2
P40	101.7	5.9	0.0	52.5	0.6	0.0	0.0	0.2
P41	108.1	0.8	0.0	52.9	0.6	0.0	0.0	0.2
P42	107.8	2.1	0.0	52.5	0.6	0.0	0.0	0.2
P43	103.5	8.5	0.0	52.9	0.6	0.0	0.0	0.2
P44	108.6	8.8	0.0	52.5	0.7	0.0	0.0	0.2
P45	125.3	−8.5	0.0	55.2	0.8	0.9	0.0	0.6
P46	103.2	0.1	0.0	44.4	0.9	0.0	0.0	0.3
P47	99.9	−6.8	0.0	41.5	0.9	0.7	0.0	0.5
P48	131.2	24.0	0.0	81.3	0.3	0.0	0.0	0.1
P49	152.9	25.2	0.0	92.1	0.3	0.0	0.0	0.1
P50	166.1	36.0	0.0	96.0	0.4	0.0	0.0	0.1
PMP1D	229.2	−10.0	2.1	100.5	0.8	1.0	0.0	0.6
PMP1S	54.4	3.0	0.0	19.8	1.2	0.0	0.0	0.4
PS1	39.3	3.0	0.0	19.8	0.6	0.0	0.0	0.2
VLV1D	114.9	−2.4	0.0	63.4	0.5	0.2	0.0	0.2
VLV1U	115.0	−2.2	0.0	63.5	0.5	0.2	0.0	0.2

level is also reasonable. From the analysis above, it can be concluded that the pipe burst risk state assessment and classification techniques proposed are correct and reliable.

As demonstrated in Tables 1 and 2, nodes J1 and J19 are the cavitation points. If water hammer protection facilities are placed at nodes J1 and J19, the hazards of a water hammer can be greatly reduced. From Tables 3 and 4 we can get that after setting a hydropneumatic tank at J1, and a surge tank at J19, the hydraulic transient simulation was performed again to confirm that the entire system is in a safe condition and not under the threat of a water hammer, except for the pipes and nodes at the side of pump suction with slight warning level.

Example 2

This example models the pipe network system of a city in China. The city has a population of 9 million, the water supply quantity is 800,000 m^3/day, the length of the pipe network is 1,200 km, and the water service area is 350 square kilometers (km^2). The pipe network system consists of 50,255 pipes that are larger than 100 mm, 49,537 nodes, 6 water treatment plants, and 27 pumps. To reduce the time of the simulation and simplify the water hammer analysis, the pipe network system was trimmed by deleting the branch pipes and merging the series nodes methods. The simplified network contains 7,082 pipes, 6,359 nodes, and 996 km of pipes. For the simplified model, five DN1000-DN1200 butterfly valves were set in five locations in the center (P-31149), east (P-31298), west (P-31135), north (P-38339), and south (P-38426). The analysis scenarios were designed to simulate pump startup and shutdown, and valves opening and closing.

Based on the water hammer risk analysis, the urban water supply network pipe burst risk classification map was created as shown in Fig. 2. As demonstrated in the figure, there is a large red area in the eastern part, especially in the southeastern corner of the city. There are some smaller areas of red in the center of the city, around the northern water plant, and near the western water plant. The rest of the city should be safe from pipe burst threats due to water hammer, but a more detailed analysis with the small area based on the district metered area (DMA) may show other problems.

The areas marked by double circles in the northeastern part of the city indicate the new development zone. There are new residents and hence additional water demands. These demands increased the water flow velocity and head loss in pipes of the

Table 3. Pipe Burst Risk State Assessment on Nodes with Protection

Node label	Elevation (m)	Pressure (steady state) (m)	Force (steady state) (kN)	Minimum pressure (transient) (m)	Maximum pressure (transient) (m)	Vapor (trans.) (L)	Force (trans.) (kN)	R1	R2	R3	R4	R
J1	412.0	50.6	576.8	17.0	53.3	0.0	589.4	0.0	0.0	0.0	0.0	0.0
J2	395.0	66.1	1,164.5	37.3	66.6	0.0	1,164.6	0.0	0.0	0.0	0.0	0.0
J3	395.0	65.0	424.6	41.5	65.4	0.0	426.2	0.0	0.0	0.0	0.0	0.0
J4	386.0	73.0	509.3	54.3	73.8	0.0	509.3	0.0	0.0	0.0	0.0	0.0
J5	380.0	77.6	524.3	66.5	78.7	0.0	524.6	0.0	0.0	0.0	0.0	0.0
J6	420.0	36.6	325.6	31.7	37.3	0.0	326.1	0.0	0.0	0.0	0.0	0.0
J7	395.0	63.2	391.1	40.9	63.5	0.0	391.1	0.0	0.0	0.0	0.0	0.0
J8	395.0	63.2	240.4	40.9	63.4	0.0	240.4	0.0	0.0	0.0	0.0	0.0
J9	395.0	61.4	430.0	42.0	61.5	0.0	430.0	0.0	0.0	0.0	0.0	0.0
J10	395.0	60.8	54.6	42.5	60.9	0.0	54.6	0.0	0.0	0.0	0.0	0.0
J11	410.0	45.6	156.7	27.6	45.6	0.0	156.7	0.0	0.0	0.0	0.0	0.0
J12	420.0	35.3	131.7	17.8	35.3	0.0	131.7	0.0	0.0	0.0	0.0	0.0
J13	390.0	65.2	202.5	47.0	65.1	0.0	202.5	0.0	0.0	0.0	0.0	0.0
J14	396.0	59.3	194.1	41.9	59.2	0.0	194.1	0.0	0.0	0.0	0.0	0.0
J15	397.0	58.2	281.9	40.7	58.1	0.0	281.9	0.0	0.0	0.0	0.0	0.0
J16	397.0	58.1	226.7	40.5	58.1	0.0	226.7	0.0	0.0	0.0	0.0	0.0
J17	380.0	74.6	358.2	57.0	74.4	0.0	358.2	0.0	0.0	0.0	0.0	0.0
J18	420.0	34.6	356.5	16.9	34.5	0.0	357.0	0.0	0.0	0.0	0.0	0.0
J19	435.0	19.6	279.5	0.2	19.5	0.0	281.4	0.0	0.0	0.0	0.0	0.0
J20	410.0	44.5	158.0	26.5	44.4	0.0	158.0	0.0	0.0	0.0	0.0	0.0
J21	385.0	67.1	185.8	50.5	66.8	0.0	185.8	0.0	0.0	0.0	0.0	0.0
J22	395.0	57.3	255.0	40.2	57.0	0.0	255.0	0.0	0.0	0.0	0.0	0.0
J23	396.0	56.4	186.1	38.6	56.1	0.0	186.1	0.0	0.0	0.0	0.0	0.0
J24	397.0	55.4	163.2	37.6	55.2	0.0	163.2	0.0	0.0	0.0	0.0	0.0
J25	408.0	44.6	85.7	27.2	44.4	0.0	85.7	0.0	0.0	0.0	0.0	0.0
J26	390.0	60.3	140.3	43.7	59.8	0.0	140.3	0.0	0.0	0.0	0.0	0.0
J27	395.0	53.9	171.2	37.3	53.1	0.0	171.2	0.0	0.0	0.0	0.0	0.0
J28	396.0	53.2	79.1	36.3	52.4	0.0	79.1	0.0	0.0	0.0	0.0	0.0
J29	396.0	53.3	51.4	36.3	52.5	0.0	51.4	0.0	0.0	0.0	0.0	0.0
J30	396.0	53.7	100.8	36.5	52.9	0.0	100.8	0.0	0.0	0.0	0.0	0.0
J31	396.0	53.3	93.9	36.2	52.5	0.0	93.9	0.0	0.0	0.0	0.0	0.0
J32	397.0	52.0	103.2	35.0	51.3	0.0	103.2	0.0	0.0	0.0	0.0	0.0
J33	410.0	41.8	100.5	24.8	41.5	0.0	100.5	0.0	0.0	0.0	0.0	0.0
J34	420.0	29.1	77.5	13.6	28.6	0.0	77.5	0.0	0.0	0.0	0.0	0.0
J35	372.0	81.5	61.7	64.0	81.3	0.0	61.7	0.0	0.0	0.0	0.0	0.0
J36	360.0	92.4	70.0	75.0	92.1	0.0	70.0	0.0	0.0	0.0	0.0	0.0
J37	355.0	96.3	42.7	79.1	96.0	0.0	42.7	0.0	0.0	0.0	0.0	0.0
PJ1	363.0	19.8	140.8	12.4	32.8	0.0	142.1	0.3	0.0	0.0	0.0	0.1
PJ2	363.0	99.8	166.9	64.5	102.4	0.0	167.2	0.0	0.0	0.0	0.0	0.0

Table 4. Pipe Burst Risk State Assessment on Pipes with Protection

Pipe label	Minimum pressure (transient) (m)	Maximum pressure (transient) (m)	Vapor (transient) (L)	Pressure (steady state) (m)	R1	R2	R3	R
P1	102.4	17.0	0.0	100.5	0.0	0.0	0.0	0.0
P2	66.6	17.0	0.0	66.6	0.0	0.0	0.0	0.0
P3	66.6	37.3	0.0	66.6	0.0	0.0	0.0	0.0
P4	73.8	41.5	0.0	73.4	0.0	0.0	0.0	0.0
P5	78.7	54.3	0.0	77.7	0.0	0.0	0.0	0.0
P6	78.7	31.7	0.0	77.7	0.0	0.0	0.0	0.0
P7	37.3	3.0	0.0	36.7	0.0	0.0	0.0	0.0
P8	66.6	37.3	0.0	66.6	0.0	0.0	0.0	0.0
P9	63.4	40.9	0.0	63.4	0.0	0.0	0.0	0.0
P10	65.1	42.0	0.0	65.1	0.0	0.0	0.0	0.0
P11	61.5	42.0	0.0	61.5	0.0	0.0	0.0	0.0
P12	60.9	27.6	0.0	60.9	0.0	0.0	0.0	0.0
P13	45.6	17.8	0.0	45.6	0.0	0.0	0.0	0.0
P14	74.4	47.0	0.0	74.4	0.0	0.0	0.0	0.0
P15	61.5	41.9	0.0	61.5	0.0	0.0	0.0	0.0
P16	59.2	40.7	0.0	59.2	0.0	0.0	0.0	0.0
P17	58.1	27.6	0.0	58.1	0.0	0.0	0.0	0.0
P18	58.1	40.5	0.0	58.1	0.0	0.0	0.0	0.0
P19	58.1	17.8	0.0	58.1	0.0	0.0	0.0	0.0
P20	74.4	50.5	0.0	74.4	0.0	0.0	0.0	0.0
P21	74.4	16.9	0.0	74.4	0.0	0.0	0.0	0.0
P22	59.2	16.9	0.0	59.2	0.0	0.0	0.0	0.0
P23	57.0	16.9	0.0	57.0	0.0	0.0	0.0	0.0
P24	34.5	0.2	0.0	34.5	0.0	0.0	0.0	0.0
P25	58.1	0.2	0.0	58.1	0.0	0.0	0.0	0.0
P26	56.1	0.2	0.0	56.1	0.0	0.0	0.0	0.0
P27	55.2	0.2	0.0	55.2	0.0	0.0	0.0	0.0
P28	44.4	0.2	0.0	44.4	0.0	0.0	0.0	0.0
P29	58.1	26.5	0.0	58.1	0.0	0.0	0.0	0.0
P30	44.4	26.5	0.0	44.4	0.0	0.0	0.0	0.0
P31	66.8	43.7	0.0	66.8	0.0	0.0	0.0	0.0
P32	66.8	40.2	0.0	66.8	0.0	0.0	0.0	0.0
P33	57.0	37.3	0.0	57.0	0.0	0.0	0.0	0.0
P34	57.0	38.6	0.0	57.0	0.0	0.0	0.0	0.0
P35	56.1	36.5	0.0	56.1	0.0	0.0	0.0	0.0
P36	56.1	37.6	0.0	56.1	0.0	0.0	0.0	0.0
P37	55.2	27.2	0.0	55.2	0.0	0.0	0.0	0.0
P38	59.8	37.3	0.0	59.8	0.0	0.0	0.0	0.0
P39	53.1	36.3	0.0	53.1	0.0	0.0	0.0	0.0
P40	52.5	36.3	0.0	52.5	0.0	0.0	0.0	0.0
P41	52.9	36.3	0.0	52.9	0.0	0.0	0.0	0.0
P42	52.5	36.2	0.0	52.5	0.0	0.0	0.0	0.0
P43	52.9	36.2	0.0	52.9	0.0	0.0	0.0	0.0
P44	52.5	35.0	0.0	52.5	0.0	0.0	0.0	0.0
P45	55.2	35.0	0.0	55.2	0.0	0.0	0.0	0.0
P46	44.4	24.8	0.0	44.4	0.0	0.0	0.0	0.0
P47	41.5	13.6	0.0	41.5	0.0	0.0	0.0	0.0
P48	81.3	57.0	0.0	81.3	0.0	0.0	0.0	0.0
P49	92.1	64.0	0.0	92.1	0.0	0.0	0.0	0.0
P50	96.0	75.0	0.0	96.0	0.0	0.0	0.0	0.0
PMP1D	104.6	63.7	0.0	100.5	0.0	0.0	0.0	0.0
PMP1S	45.5	7.4	0.0	19.8	0.8	0.0	0.0	0.3
PS1	32.8	3.0	0.0	19.8	0.3	0.0	0.0	0.1
VLV1D	63.4	40.9	0.0	63.4	0.0	0.0	0.0	0.0
VLV1U	63.5	40.9	0.0	63.5	0.0	0.0	0.0	0.0

old town located at the southeastern corner of the city; therefore, high positive pressure occurs in that area. Another reason is that the ground elevation of the old town is higher than the other parts, and there is a water tank that has water mains connected in the middle of the red area. So negative pressure and cavitation easily occurred in that area. Therefore, the large red area is reasonable from the analysis of pipe burst risk state assessment and classification techniques proposed.

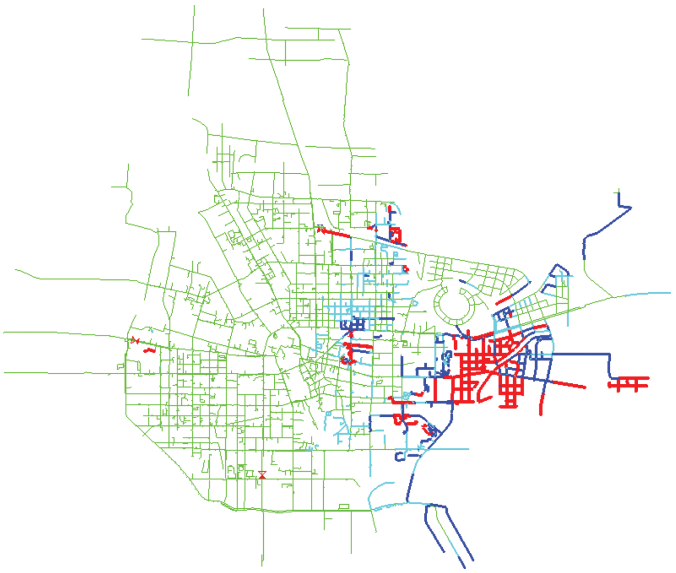

Fig. 2. (Color) Water hammer risk maps for example 2

Conclusions and Recommendations

A pipe burst can destroy a city's pipe network, leading to water supply interruption, loss of life and property, as well as water quality problems. Pipe burst risk assessment and classification technology based on water hammer analysis for water supply networks can estimate the approximate time that a pipe will be out of service and can easily formulate a pipe network maintenance plan in advance to avoid the occurrence of burst pipes. Based on hydraulic transient flow analysis, pipe burst risk factors are predicted for maximum water pressure, maximum vacuum, maximum vapor volume, and maximum transient force. The composite risk factor also can be calculated by the above four factors. The color coding map can be created based on the four-layer state assessment technology of Class I (green), Class II (cyan), Class III (blue), and Class IV (red). The method and technology are verified by two examples. The results show that the research methods can provide technical support for the design, operation, and management of water supply networks.

For severe water hammer damage to a water supply pipe network, the following need to be considered when using the techniques:

1. The computer model system can not only improve work efficiency, but can also provide technical support for the operation and maintenance of a water supply network from the height of the entire network economically;
2. Water hammer hazard assessment can determine risk classification and point out potential problem areas where the water supplier can implement actions to prevent or minimize water hammer;
3. Regularly carry out the pipe burst risk state assessment and classification planning;
4. Monitoring and inspecting the severe level areas, and reserving the appropriate tools and supplies there;
5. Selecting the weight of the risk factors reasonably according to the actual situation. For example, a large weight of vapor volume risk factor should be considered when selecting the water

hammer protection equipment installing locations, while a small weight of vacuum risk factor should be considered when the pipe material is concrete.

6. Pipes break for a lot of reasons, such as incorrect external loading, contact with backhoes and other equipment, poor materials, corrosion, seasonal factors, etc. The technique we proposed only works for pipes that burst due to hydraulic transients.

Acknowledgments

The authors acknowledge the financial support of the Shenzhen Fundamental Research Program of China "Water supply network pipe burst and leakage control technology research (JC20110 5180804A)" and "Water supply network optimization scheduling technology research (JCYJ20120616213618826)," and Seventh Framework Programme (FP7) Marie Curie Actions (PIRSES-GA-2012-318985).

References

Arbon, N. S., Lambert, M. F., Simpson, A. R., and Stephens, M. L. (2007). "Field test investigations into distributed fault modeling in water distribution systems using transient testing." *Proc., World Environmental and Water Resources Congress 2007*, ASCE, Reston, VA.

Colombo, A. F., Lee, P., and Karney, B. W. (2009). "A selective literature review of transient-based leak detection methods." *J. Hydro-environ. Res.*, 2(4), 212–227.

Ebacher, G., Besner, M. C., Prévost, M., and Allard, D. (2011). "Negative pressure events in water distribution systems: Public health risk assessment based on transient analysis outputs." *Water distribution systems analysis 2010*, ASCE, Reston, VA.

Ghidaoui, M. S., Zhao, M., and McInnis, D. A. (2005). "A review of water hammer theory and practice." *Appl. Mech. Rev.*, 58(1), 49–76.

Gong, J., Simpson, A. R., Lambert, M. F., Zecchin, A. C., Kim, Y., and Tijsseling, A. S. (2013). "Detection of distributed deterioration in single pipes using transient reflections." *J. Pipeline Syst. Eng. Pract.*, 10.1061/(ASCE)PS.1949-1204.0000111, 32–40.

Grigg, N. (2013). "Water main breaks: Risk assessment and investment strategies." *J. Pipeline Syst. Eng. Pract.*, 10.1061/(ASCE)PS.1949-1204.0000142, 04013001.

Haestad Methods Water Solutions. (2013). *Bentley HAMMER V8i SS3 user's guide*, Bentley Systems.

Horsburgh, J. S., et al. (2009). "An integrated system for publishing environmental observations data." *Environ. Modell. Software*, 24(8), 879–888.

Kanta, L., and Brumbelow, K. (2013). "Vulnerability, risk, and mitigation assessment of water distribution systems for insufficient fire flows." *J. Water Resour. Plann. Manage.*, 10.1061/(ASCE)WR.1943-5452.0000281, 593–603.

Kim, J., et al. (2012). "Assessment of the behavior of buried concrete pipelines subjected to ground rupture: Experimental study." *J. Pipeline Syst. Eng. Pract.*, 10.1061/(ASCE)PS.1949-1204.0000088, 8–16.

Kroll, D. (2010). "Criteria for evaluating distribution network early warning systems." *World Environmental and Water Resources Congress 2010: Challenges of Change*, ASCE, Reston, VA, 428–447.

Lee, P. J., Lambert, M. F., Simpson, A. R., Vítkovský, J. P., and Misiunas, D. (2007). "Leak location in single pipelines using transient reflections." *Aust. J. Water Resour.*, 11(1), 53–65.

Livingston, B., Boudjou, U., and Royer, R. (2012). "Condition assessment of a ductile iron force main using guided wave technology: Case study of Underwood Creek force main, Milwaukee metropolitan sewerage district." *Pipelines 2012: Innovations in Design, Construction, Operations, and Maintenance, Doing More with Less*, ASCE, Reston, VA, pp. 442–456.

Mehrooz, M., Kirkwood, G. C., Scheinman, S., and Bayer, G. T. (2007). "Corrosion sensors for detecting graphitization of cast iron in water mains." *Corrosion 2007*, National Association of Corrosion Engineers (NACE) International, Houston, TX.

Mutikanga, H., Sharma, S., and Vairavamoorthy, K. (2013). "Methods and tools for managing losses in water distribution systems." *J. Water Resour. Plann. Manage.*, 10.1061/(ASCE)WR.1943-5452.0000245, 166–174.

Ostfeld, A., and Salomons, E. (2004). "Optimal layout of early warning detection stations for water distribution systems security." *J. Water Resour. Plann. Manage.*, 10.1061/(ASCE)0733-9496(2004)130:5(377), 377–385.

Rajani, B., and Kleiner, Y. (2013). "External and internal corrosion of large-diameter cast iron mains." *J. Infrastruct. Syst.*, 10.1061/(ASCE)IS.1943-555X.0000135, 486–495.

Romano, M., and Kapelan, Z. (2011). "Burst detection and location in water distribution systems." *World Environmental and Water Resources Congress 2011: Bearing Knowledge for Sustainability*, ASCE, Reston, VA, 1–10.

Rossman, L. A. (2000). *EPANET 2: User's manual*, National Risk Management Research Laboratory, Cincinnati. OH.

Stephens, M. L., Lambert, M. F., Simpson, A., and Vitkovsky, J. (2011). "Calibrating the water-hammer response of a field pipe network by using a mechanical damping model." *J. Hydraul. Eng.*, 10.1061/(ASCE)HY.1943-7900.0000413, 1225–1237.

Wang, R., et al. (2013). "Hydraulic transient prevention with dipping tube hydropneumatic tank." *Appl. Mech. Mater.*, 316, 762–765.

Wang, R., Wang, Z., Walski, T. M., Sharkey, M., Coran, S. R., and Zemell, S. H. (2011). "Modeling of hydraulic transient control with vented hydropneumatic tank." *11th Int. Conf. on Computing and Contgrol for Water Industry (CCWI 2011)*, Exeter, U.K., 877–882.

Xiong, S., Guan, X., and Jin, Z. (2003). "Problems and design example of comprehensive protection for water hammer due to cavities collapsing with water column separation at multi-points." *Water Wastewater Eng.*, 29(7), 1–5 (in Chinese).

Zhang, F., Wang, R., Yang, H., Wang, X., and Luo, J. (2012). "Development and application of early warning system for drinking water security in Dongguan, China." *World Environmental and Water Resources Congress 2012: Crossing Boundaries*, ASCE, Reston, VA, 720–728.